Isochromatic Demodulation by Fringe Scanning

G. S. Grewal, V. N. Dubey and D. J. Claremont

School of Design, Engineering & Computing, Bournemouth University, Talbot Campus, Fern Barrow, Poole BH12 5BB, UK

ABSTRACT: RGB calibration is the fastest isochromatic demodulation technique, as it does not require unwrapping as in the case of phase-shifting method. The technique is based on constructing a look up table (LUT) of fringe order against RGB triplet from digital images and decoding the test image from the LUT. Research has shown that the technique, though very fast, is limited to fringe orders up to three with the conventional white light. The colours tend to merge beyond that and make it difficult to obtain a unique value of RGB triplet. Changes in fringe gradient caused by stretching/bunching of fringes in test model further add to errors. Special light sources with narrow-band spectral response are required with fringe tracking algorithms to demodulate higher fringe orders. The calibration technique is also sensitive to geometric and chromatic variations. This paper presents a cost-effective alternative solution to conventional RGB technique using a flatbed scanner. The system is capable of demodulating higher fringe order and incorporates information from other colour spaces. It does not require separate light sources and cameras, and is found to be insensitive to geometric and chromatic variations. Curve fitting technique has been proposed to determine accurate fringe orders.

KEY WORDS: *fringe demodulation, image unwrapping, LUT-based calibration, RGB photoelasticity, stress analysis*

Introduction

Photoelasticity is a well-established optical technique for stress analysis. A number of techniques have been developed over the years to accurately analyse the data available from photoelastic fringe patterns. Two well-known techniques are phase-shifting [1, 2] and RGB calibration [3–7]. Phase-shifting is one of the most promising techniques, although it requires expensive equipment and considerable computational time in phase unwrapping. A few portable systems based on phase-shifting are available commercially for stress analysis [8, 9], but surprisingly there are no such systems available for RGB calibration. The reasons may be that the technique is sensitive to fringe gradient, geometric and chromatic parameters, and requires *in situ* calibration. The RGB calibration technique uses a look up table (LUT) which has entries of fringe order against unique RGB triplet values. Once the calibration is done, isochromatic values for a point in the sample is determined by search based on minimum Euclidean distance between the measured RGB triplet and the RGB value from the calibration database. Thus, fringe order can be estimated and stress analysis can be performed. This paper discusses the traditional RGB calibration method as a ready reference for implementation purposes, and proposes a new technique based on other colour spaces using scanner technology which is largely independent of geometric and chromatic variations. The paper also presents advantages of the proposed method over other existing techniques.

RGB Calibration Procedure

RGB calibration method requires a diffused light source, a digital camera and a polariscope. The experimental environment is constrained with regard to distance between camera, model and light source, and the type of light source used. The method requires that the geometrical and optical parameters be kept constant during calibration and analysis; changes can lead to inaccurate results. Typically, the calibration procedure involves a C-shaped photoelastic model under bending load. From the geometry of the model and the loading conditions shown in Figure 1A, it is evident that the central section of the model is under uniform loading and the transverse line (a–b) across the section has linear distribution of stresses. This can be seen in the fringe pattern in Figure 1B. The black fringe represents the zero fringe order falling nearly over the neutral axis with increasing stresses on both sides. As the middle

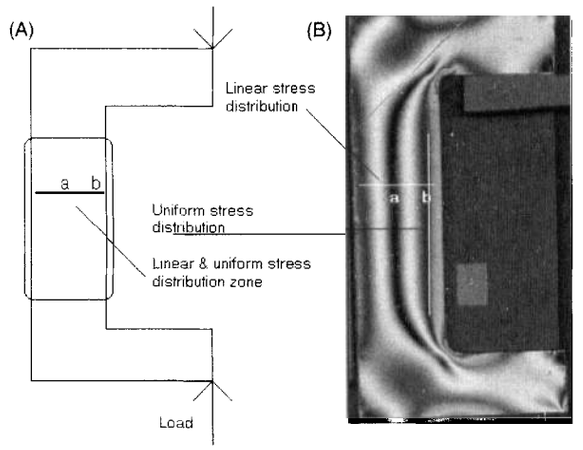

Figure 1: Model under bending load for the calibration database

section has uniform and linear stress distribution (rectangular area in the figure) this area is regarded as the region of interest (ROI).

Appropriate bending load was applied to the model to induce a known fringe order (N) against the fringe colour. The fringe order is available from the standard isochromatic colour characteristics [5, 10]. The RGB image of the developed fringe pattern was captured using a high-resolution digital camera (8-bit Fuji FinePix s7000, Fuji Photo Film, Valhalla, NY, USA). The images were then transferred to a personal computer for further processing. The ROI in the image was filtered using a 'mean-filter' to remove electronic noise and to smooth the image; as CCD is highly sensitive to intensity changes. A transverse calibration line 'a–b' (Figure 1) was selected in the ROI with linear stress distribution and RGB triplet values were recorded. The line has a start point at the middle of the neutral axis with zero fringe order (black fringe), and fringe order (N) at the end point. Thus the first pixel corresponds to zero fringe order and the successive fringe orders can be calculated by the following linear scaling (Equation 1):

$$N_i = N\frac{i}{n}, \tag{1}$$

where N is maximum relative retardation induced, N_i is retardation at required pixel, i is pixel number, and n is total number of pixels in the selected line.

The above steps were repeated for 50 transverse lines and the averaged results were saved in a calibration database – this helped in further noise removal and making the calibration table robust. The whole process was repeated with different values of maximum fringe order by changing the bending load. For analysis up to fringe order 3, a minimum of three different calibration databases were built ranging from fringe orders 0–1, 0–2 and 0–3. Thus the number of calibration tables required depended on maximum expected fringe order in the test model.

Fringe Analysis

As the calibration database was built with RGB triplet against fringe order, analysis was carried out for sample points on test specimen to determine retardation and the corresponding stress difference. The RGB triplet was measured at the point of interest in the test specimen and a search was performed to compare this with the stored RGB triplets in the calibration database. As all the possible RGB triplet values cannot be included in the LUT for various factors including changes due to high sensitivity of CCDs, material properties, and fringe gradient, an Euclidean square function (e) was used to determine the closest match of RGB triplet in the database using:

$$e = (R_i - R_m)^2 + (G_i - G_m)^2 + (B_i - B_m)^2 \tag{2}$$

where (R, G, B) is the stored triplet value in the calibration table, 'i' is the index in the calibration table, and (R_m, G_m, B_m) is the measured RGB triplet value.

Equation (2) gives the square error of RGB triplet between the calibration data and the measured RGB triplet of the test point. Fringe order of RGB triplet with minimum e from LUT is designated as the retardation for the test point. Using commercially available white light source, the results can be quite erroneous even by the Euclidean approach (as explained below), thus a robust algorithm is required to cope with this problem. The most common technique uses piecewise continuity to keep a track of the determined fringe orders.

Factors for Analysis

Although the above procedures appear to be simple and straightforward, there are many parameters that need to be considered for building precise calibration databases. For example, circular polariscope setup uses quarter wave plates that are designed for specific wavelength only. Such plates are efficient for stress analysis using monochromatic light source, but they introduce errors with white light. As white light is composed of a wide range of wavelengths, use of conventional quarter wave plates is incapable of introducing 'quarter-shift' to all the wavelengths, thus introducing errors in calculations. These errors

cannot be eliminated completely in circular polariscope arrangement without using achromatic quarter wave plates, but can be minimised if calibration is performed at isoclinics of 22.5°. It has been shown that plates at this angle introduce minimum errors [11].

The RGB calibration is sensitive to both geometric and chromatic parameters. Geometric parameters include distance between specimen and the light source, camera aperture and are also influenced by any light variations in the experimental setup. Chromatic parameters depend on spectral response of light source, spectral absorption of specimen and thickness of the model. Research has shown that it is difficult to control chromatic parameters compared with geometric parameters [6, 7]; however, geometric parameters can be refined by implementing *r*, *g*, *b* instead of R, G and B. The *r*, *g*, *b* are computed by normalising the RGB triplet values. Though they account for geometric variations to some extent but generate erroneous results at low fringe orders due to noise amplification [3, 5, 7]. This can be further improved by background subtraction to minimise the geometric variations of non-uniform illumination – a base image under zero-load is subtracted from each image under analysis and also during calibration procedure. However, the background subtraction may not be an ideal approach if model deformation is high [5].

Most digital cameras support only 8-bit (0–255) image acquisition per channel.[1] If a calibration database is built using 10-bit image (0–1023) per channel, the minimum search-error can be improved as the resolution is much higher. Another approach is to calibrate at higher pixel resolution (say 4 million) and perform analysis at lower resolution (say 2 million). Calibrating at 4 million pixels will include more values of RGB triplets and thus minimising the errors. As all the possible RGB triplet values against fringe order cannot be obtained and stored in the database, building more than one calibration database will account not only for the resolution issue but also for the varying fringe gradient. It is also important to note that calibration is performed on a linear fringe variation but in many cases the test specimen will have non-linear stress distribution and different fringe gradient. Therefore, more than one calibration database may be necessary. Calibration database can be built for both light field and dark field polariscope setup, thus further minimising the errors in the final results [5]. However, this approach makes the system less dynamic as it requires two images with different optical orientations. Selecting appropriate light intensity is important for the quality of images, however, care must be taken to avoid saturation of RGB planes by too high intensity so that the colour information is not lost. It is important to account for these factors in order to build robust and accurate calibration databases. Besides these, care must also be taken for camera settings which include appropriate zoom, focus and aperture value. The whole procedure is rather complex and needs a controlled environment.

[1]R, G and B channels.

Fringe Acquisition

To resolve some of the above issues, a rather unconventional approach was adopted for RGB calibration. The technique uses a commercially available flatbed scanner, EPSON® Perfection 1660 PHOTO (Epson America, Long Beach, CA, USA), which uses white cold cathode fluorescent lamp. The RGB spectrum for this light source is shown in Figure 2, clearly the scanner has a narrow band with highest spectral response in the green-yellow region representing the white light [12], which is suitable for demodulating higher fringe orders [13].

The above-discussed calibration procedure was used with this scanner to produce high quality images and LUT. This eliminated the need for expensive and separate imaging devices, meeting all the high-end specifications of the technique. Use of flatbed scanner in phase-shifting photoelasticity has been reported [14] which required a series of phase-stepped images. The reported system appeared to be bulky and complex with rotating holders which rendered it untenable in practical systems. In addition, the system could only be applied to transparent models in either static or frozen stress condition; this limited the application of phase-shifting technique for majority of real parts using the scanner. This paper presents RGB calibration technique using a scanner in reflec-

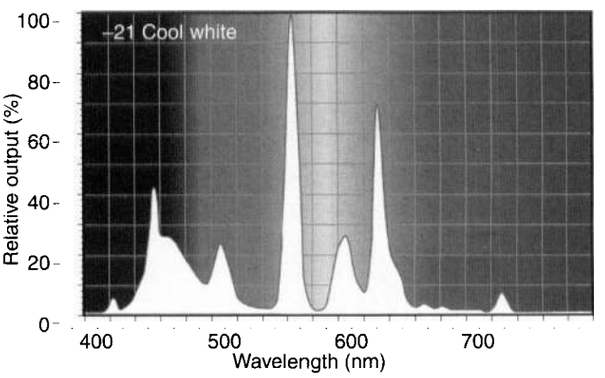

Figure 2: RGB spectrum of the scanner used in the experiment

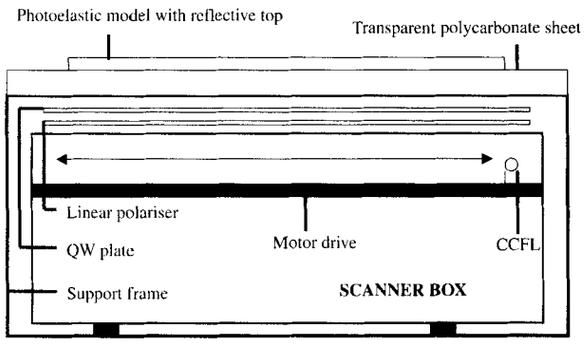

Figure 3: Scanner setup for the photoelastic experiment

tion mode which can be applied to non-transparent objects and it just requires one image per analysis. The scanner setup is shown in Figure 3, where polariser and quarter wave plate are directly placed over the scanner bed followed by the model on a support frame with a transparent polycarbonate sheet. The placing of polariser, quarter wave plate and spacing between scanner bed and the model is slightly exaggerated in the figure, which might appear to be affecting the depth of field of the scanner [15]. However, as long as the thickness of the model is uniform throughout, consistent result can be achieved; focus of the scanner can be changed by controlling the aperture if required during experimentation. The setup is ideally suited for stress-frozen models placed directly over the scanner bed, however, the scanner with polariser and quarter wave plate can be held up against the model in case of large or clamped models.

A well-diffused high-power compact fluorescent light source with uniform illumination was used in the experimental setup 1 as shown in Table 1, for comparison with the scanner output. The RGB signals along a calibration line were obtained from the two experimental setups with the above calibration procedure. The output of RGB profile was taken over 50 transverse calibration lines and averaged data were plotted. Figure 4A shows the ROI for the model under a bending load and Figure 4B is the RGB signals along the calibration line using the fluorescent light for a maximum fringe order of 4. The RGB signals extend over a range of 0–255 but as can be seen from the figure, signals tend to attenuate with the increasing fringe order making it difficult to identify the RGB

Table 1: Optical components of experimental setups

Setup	Light source	Camera	Illumination
1	Fluorescent lamp	Fuji s7000 (6.3M)	Diffused
2	Scanner-integrated	Scanner-integrated	Cold cathode fluorescent lamp

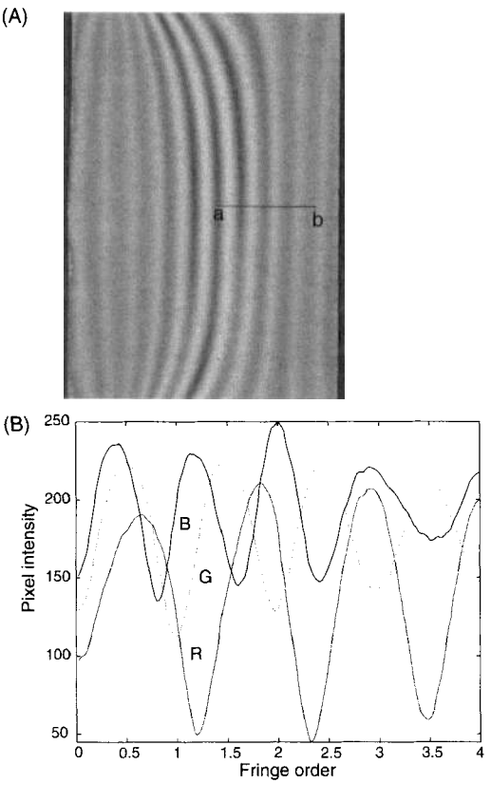

Figure 4: Fringe pattern with fluorescent light and the corresponding RGB signals along line 'a–b'

triplets. To overcome the problem of RGB signal attenuation special light sources can be used with narrow bandwidth and high-spectral response but this adds to cost and the setup size.

Using a scanner high quality image and low RGB signal attenuation can be achieved. Figure 5A shows the image acquired using the scanner. It can be seen that the image quality is better than the previous case. Figure 5B shows the RGB signal profile across the calibration line a–b. Figures 4 and 5 clearly show that scanner system will demodulate higher fringe orders and provide better LUT when compared with the conventional light sources due to low signal attenuation. This gives a significant advantage for the RGB calibration method to achieve higher fringe orders with such a simple approach. Further, it can be seen (Figure 5) that the blue intensity signal is attenuating more rapidly when compared with red and green signals as reported in Ng *et al.* [14]; a custom-made scanner with appropriate light source can overcome this problem. Even though the scanner provides high spectral response for RGB signals, the ambiguity of fringe order due to colour repetition still needs to be resolved. A robust algorithm to keep the track of fringe order by incorporating information from previously demodulated points needs to be developed to account for this [3, 7].

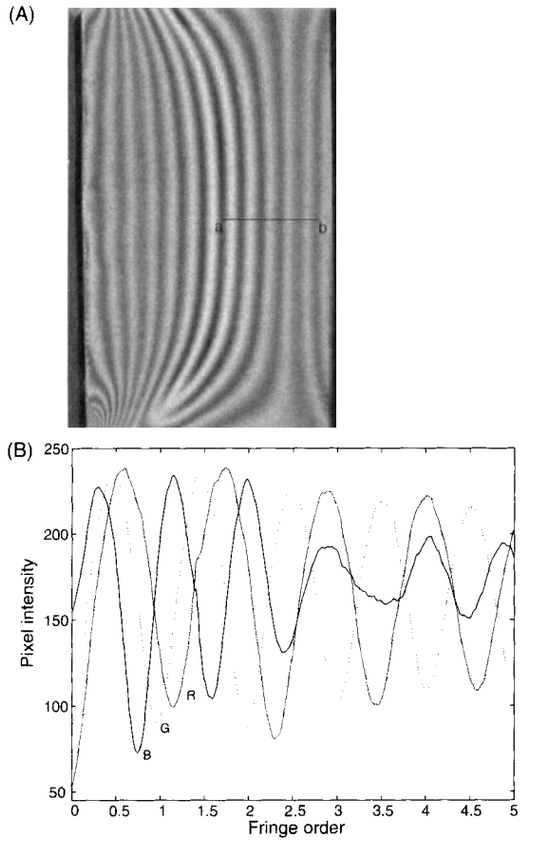

Figure 5: Fringe pattern with scanner and the corresponding RGB signal along line 'a–b'

Calibration Database and Resolution

The final LUT is usually limited by resolution and the bit-value of the image acquired for data extraction. In order to generate an accurate and robust LUT it is essential that a camera with higher resolution and bit-value should be used, which adds to cost and effort. The approach presented here does not require any of the above and is still capable of providing up to 48-bit images. A 48-bit image has 16 bits for each available channel of R, G and B thus providing 65 536 unique values per channel over 256 possible values from the conventional methods. The following section compares the capabilities of conventional method versus our technique in terms of the calibration database. The photoelastic model used to create the calibration database had the following parameters as shown in Table 2.

Resolution Mathematics

The maximum possible resolution to acquire an image will be 2848 × 2136 pixels with the Fuji s7000 camera, but the maximum permissible data points along the calibration line will be limited to much lower values (300–500 pixels) due to practical difficulties of framing such a small region. In order to achieve higher resolution on the calibration line, it would be necessary to place the camera close to the model whilst maintaining the illumination. It is worth noting that the above procedure to frame the calibration line with very high resolution is not trivial and most experimental setups are incapable of achieving this. Alternatively, one can use higher optical magnification and then frame the desired ROI, which will increase the distance between model, light and camera. With the available digital camera one can achieve a fringe resolution of 2×10^{-2} when compared with 4.5×10^{-3} from the scanner for a maximum fringe order of 4. (Note: the fringe resolution is calculated by dividing the maximum produced fringe order by the number of pixels along the calibration line.) As scanner resolution is specified as pixels per inch, increasing the size of model increases the number of effective pixels in the ROI. The scanner also offers the advantage of 16-bit channel of R, G and B when compared with 8-bit channels from the digital camera. More importantly, from these data points there were no repetitions of RGB triplets thus all of them had a unique value providing fringe orders up to 5.

Table 2: Parameters of the model material

Strain optic coefficient (K)	0.15
Modulus of elasticity (E) GPa	2.5
Poisson's ratio (ν)	0.38
Thickness (mm)	3.05
Width (mm)	30

Fringe Demodulation using Other Colour Spaces

The conventional method for fringe demodulation in RGB calibration is achieved by the Euclidean least square technique. Using Equation (2) the closest match is searched between measured RGB triplet and the stored RGB triplet and accordingly the fringe order is assigned. In order to evaluate the robustness of the least square approach it is important to visualise a three-dimensional (3D) plot of RGB calibration curve from the database. Figure 6 shows a 3D plot of RGB calibration database up to fringe order of 4, a closer inspection reveals how tightly packed the database is. A 3D curve with higher fringe orders gets even more complex and thus prone to errors. From the entire cube of RGB colour space, the database is

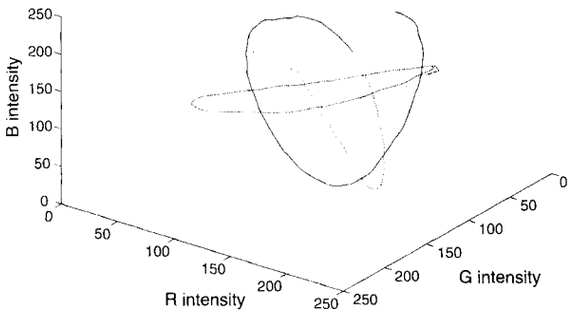

Figure 6: RGB database representation

limited only to a couple of lines which is why during analysis the test point is usually not available within the database. As seen in the figure the database is formed in the shape of helical rings close to each other. Stretching and bunching of fringe gradient further drift the test point away from its corresponding match in the database making the system prone to errors. This can be explained by assuming the *black* dot as a test point under analysis (Figure 6). During the least square search the determined fringe order can be erroneously picked up from any of the closest helix rather than the original match. Light sources with much higher spectral response can provide demodulation of higher fringe orders but will need advanced algorithms to tackle fringe order ambiguity due to the colour repetition.

In order to overcome the above problem, different representations of the colour have been tried. The colour representation involving H, $(R\text{-}G)$, $(G\text{-}B)$, $(R\text{-}B)$ gave the best results. Thus a new search with error function (e_h) involving H, $(R\text{-}G)$, $(G\text{-}B)$, $(R\text{-}B)$ was performed using Equation (3) instead of comparing the test point with the RGB triplet. As the hue component from HSV/HSI[2] images has the colour information, which represents the gradation of colour within the visible spectrum of light, change in fringe gradient or slight variation in light intensity does not change the original colour information but only the shade of the colour. Any change in R, G or B signals is minimised by the difference term rather than their absolute values. Thus choosing H, $(R\text{-}G)$, $(G\text{-}B)$ and $(R\text{-}B)$ parameters helps in minimising errors in determining higher fringe orders. For these reasons H, $(R\text{-}G)$, $(G\text{-}B)$ and $(R\text{-}B)$ become the appropriate parameters for this search. The benefit of using other colour space information for fringe demodulation depends on the fringe order to be determined; this search was found to be better suited for achieving higher fringe orders with consistent result against stretching/bunching of the fringes:

[2]Hue-Saturation-Value/Intensity.

$$\begin{aligned} e_h = {} & (H_i - H_m)^2 + [|(R_i - G_i)| - |(R_m - G_m)|]^2 \\ & + [|(G_i - B_i)| - |(G_m - B_m)|]^2 \\ & + [|(R_i - B_i)| - |(R_m - B_m)|]^2, \end{aligned} \tag{3}$$

where e_h is the new error function, (R, G, B, H) are the stored colour values in the calibration table, 'i' is the index in the calibration table, and (R_m, G_m, B_m, H_m) are the measured RGBH values.

Experimental Results and Validation

In order to test the validity and robustness of the proposed system, an analysis was performed for the problem of disc under diametral compression. Results obtained from the two systems (Fluorescent light and Scanner system) have been presented to demonstrate advantage of the scanner system.

Fluorescent Light

Figure 7A shows the disc image taken under the diffused fluorescent light source and Figure 7B is the corresponding plot obtained by the RGB Euclidean approach. The results are good up to fringe orders of 3, beyond this merging of colours occurs which cannot be resolved by this technique. Figure 8 shows

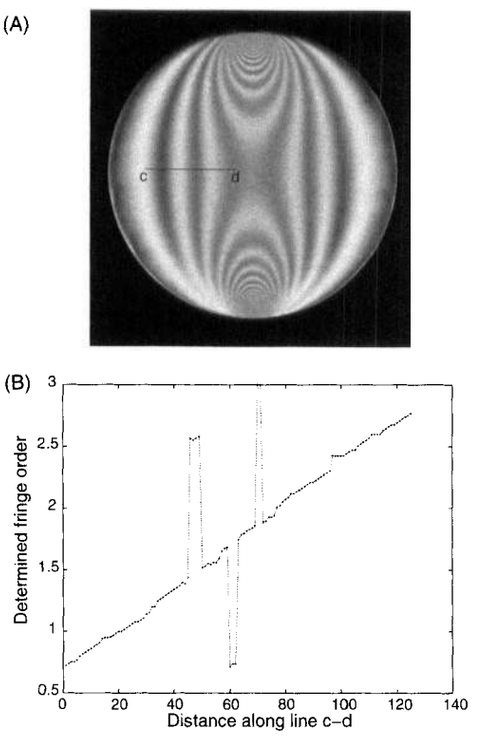

Figure 7: Test image from fluorescent light and fringe order determined by RGB match

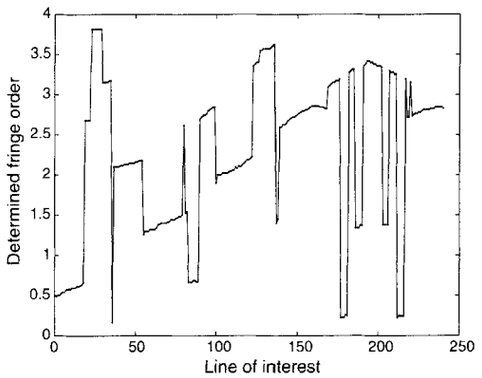

Figure 8: Fringe order ($N > 3$) determined by the RGB match

the effect of signal attenuation when higher fringe orders are demodulated for this conventional light source. Minor errors in the demodulated signals can be overcome by using piecewise continuity to suppress the errors from previously demodulated points but for a robust system advanced algorithms needs to be developed with special light sources. In the following section the scanner results with image information from other colour spaces have been compared to demodulate higher fringe orders.

Scanner

Figure 9A shows the test image acquired using the flatbed scanner. Line 'c–d' on the disc is analysed for fringe order. Due to repetition of colours and stretching/squeezing of the fringe gradient the previous technique to resolve fringe order can be prone to errors. However, when e_h function (Equation 3) was adopted for demodulation, the errors were very much suppressed as seen in Figure 9B. The scattered errors could have been further minimised if piecewise continuity was used.

To develop a robust system, a curve fitting approach was adopted to suppress the errors for demodulating higher fringe orders. A cubic polynomial was fitted to the data (excluding the scattered points) to obtain an equation for determining the fringe order. The noisy data was initially eliminated by excluding the data points falling outside 50% confidence range of a linear fit to the data (done in MATLAB®, MathWorks, Natick, MA, USA). The remaining data were then used for fitting a polynomial curve. Selecting 50% confidence range gave optimal results, where most of the noisy data were eliminated and allowed an easy polynomial fit. The technique was used to minimise the errors for a line profile on the image, which was representative of the stress variation over the model, however, for

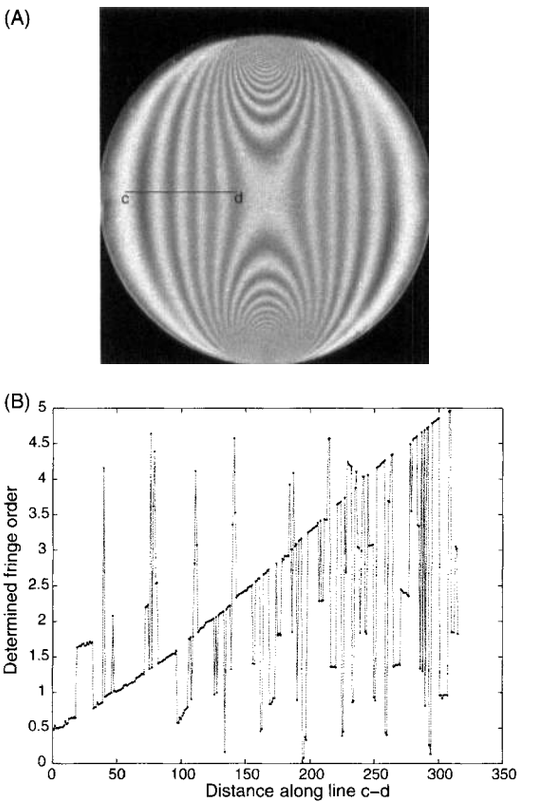

Figure 9: Test image and fringe order determined by e_h function

any irregular stress variation to cover the entire image, the same technique can be applied by splitting the entire curve into ascending and descending trends and analysing them piecewise. Equation (4) represents the polynomial curve and Figure 10 shows the polynomial curve through the data points (thick/red line through the data points). Using this equation fringe orders can be accurately determined excluding the erroneous peaks in Figure 9B:

$$N = -(7.49e-8)x^3 + (4.44e-5)x^2 + (7.99e-3)x + 0.5. \quad (4)$$

This equation can be used to find the fringe order at any point along line 'c–d' by substituting the pixel number of the point – fringe order being 0.52 at 'c' and maximum at point 'd'. In order to further verify these results, a theoretical graph was plotted along with the polynomial fit for the photoelastic disc of the same material properties (Table 2) under diametral compression. The existing analytical relation [5] was modified to find the fringe order as given by Equation (5):

$$N = \frac{8PR(1+\nu)K}{\pi\lambda E} \frac{R^2 - (x^2+y^2)}{(x^2+y^2+R^2)^2 - 4y^2R^2}, \quad (5)$$

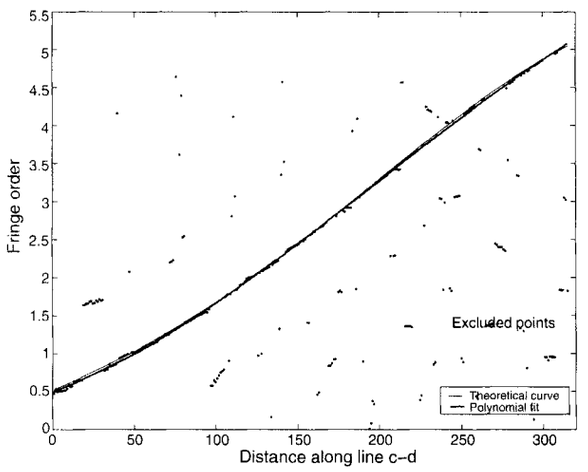

Figure 10: Comparison of theoretical and experimental fringe orders

where P is the applied load, R is the radius of the disc, ν is Poisson's ratio, E is modulus of elasticity, K is strain optic co-efficient of the material, λ is the wavelength of the light (575 nm) and x, y are the coordinates of the test points with respect to the centre of the disc.

As can be seen in Figure 10, a slight difference exists between the theoretical (thin line) and the actual curves; this is inevitable due to difference in fringe gradient of the calibration LUT and the actual test specimen. This validates our presumptions that the RGB calibration, being the fastest demodulation techniques, can be implemented effectively using a scanner. As the experimental data is very close to the theoretical curve, the determined fringe order will be accurate. In the current implementation the minimum absolute error in fringe order was found to be 8.15×10^{-4} and maximum error was 0.041. If the whole process of data fitting can be automated more accurate results can be achieved by this method.

As calibration is done on linear data and the test data is non-linear, the RGB calibration system is subject to errors when compared with the phase-shifting method. A better LUT can be developed if calibration is done using an arc-shaped model [7] – the load can be incremented in steps and the data are collected from a section of image with uniform stress, the next loading-step represents the incremental fringe order. This means slow incremental steps can provide a better LUT; also better demodulation algorithms can cope with fringe gradient changes and make systems less prone to errors.

Advantages of this Approach

Use of the flatbed scanner as an unconventional device for photoelastic fringe demodulation gave advantages in many aspects. First of all, it does not require a digital camera and can still provide resolution up to 10 million pixels per square inch (3200 dpi). More importantly, a 6M digital camera is not capable of framing 2848 pixels across the selected calibration line, and this does not require any settings such as zoom, focus, aperture or shutter speed to generate sharp images with high clarity. The image is acquired at 48-bit resolution, thus 16-bit for each plane. This provides more robust databases with higher resolution and minimum errors for the Euclidean square function. The diffused light source scans over entire model with uniform illumination and as the scanning is performed at a close proximity, this makes the system insensitive to geometric variations. Further, there is no need to devise a new experimental setup and the whole process is simple and easy to implement with no experimental constraints of light or camera settings. It is also insensitive to the surrounding light sources unlike the conventional techniques, which require great care in maintaining lighting conditions in the RGB calibration systems. Finally, because of high spectral response of the scanner, fringe order up to 5 can be easily demodulated without any special light source requirement and the system is portable, cost-effective and highly efficient. The only drawback of this approach is the time required to scan the image. Image acquisition could be time consuming and can take up to several minutes if very high resolution is required, thus choice of resolution is user dependent.

Conclusions

An approach has been presented for demodulating photoelastic fringes using a flatbed scanner. The technique uses a commercially available inexpensive scanner and yet provides better and accurate results. The setup does not require any digital cameras or light sources unlike the conventional methods, however, the images acquired are of high quality and high resolution. No settings are required for lighting and camera which are difficult to maintain in conventional systems during calibration and image acquisition phase. The calibration can be performed in easy steps without any accessories or external setup. The results presented in this paper show that image acquired and LUT were improved using the scanner and thus provide an alternative 'easy-to-implement' technique to the conventional RGB calibration. Information from other colour spaces has provided alternative search parameters, which removes ambiguity in resolving higher fringe orders

($N > 3$) without using any special light sources or resorting to complicated algorithms. A fitted polynomial through the data points could be another approach for determining accurate fringe orders in place of piecewise continuity. The proposed approach can be used as a portable system for static stress analysis, especially for research and educational purposes. The technique can also be very well suited for quick stress analysis applications in an affordable system if the entire process could be automated. Flat specimens can be directly placed on the scanner bed and for heavier parts scanner can be held up against the part for image acquisition. Comparing these aspects with the conventional RGB technique it can be concluded that this approach is simpler, efficient and cost-effective.

ACKNOWLEDGEMENT

This research was supported by a bursary offered by the School of Design, Engineering & Computing, Bournemouth University.

REFERENCES

1. Patterson, E., Pacey, M. and Haake, S. (2000) A novel instrument for automated principal strain separation in reflection photoelasticity. *J. Test. Eval.* **28**, 229–235.
2. Patterson, E. (2002) Digital photoelasticity: principles, practice and potential. *Strain* **38**, 27–39.
3. Ajovalasit, A., Barone, S. and Petrucci, G. (1995) Towards RGB photoelasticity: full-field started photoelasticity in white light. *Exp. Mech.* **35**, 193–200.
4. Ramesh, K. and Deshmukh, S. (1996) Three fringe photoelasticity-use of colour image processing hardware to automate ordering of isochromatics. *Strain* **32**, 79–86.
5. Ramesh, K. (2000) *Digital Photoelasticity: Advanced Techniques and Applications*. Springer, Berlin.
6. Quiroga, J. and Botella, A. (2001) Demodulation of isochromatic RGB fringe patterns by an improved calibration technique. *Proc. 4th Int. Workshop on Automatic Processing of Fringe Patterns*, Paris, France: 126–133.
7. Quiroga, J., Botella, A. and Gomez-Pedrero, J. (2002) Improved method for isochromatic demodulation by RGB calibration. *Appl. Optics* **41**, 3461–3468.
8. Patterson, E., Hobbs, J. and Greene, R. (2003) A novel instrument for transient photoelasticity. *Soc. Exp. Mech.* **43**, 403–409.
9. Lesniak, J. R., Zhang, S. J. and Patterson, E. A. (2004) The design and evaluation of the poleidoscope: a novel digital polariscope. *Exp. Mech.* **44**, 128–135.
10. Vishay Measurement Groups (1989) *Introduction to Stress Analysis by the Photostress Method, Tech Note, TN-702-1*. Vishay Measurement Groups, Raleigh, NC, USA.
11. Ajovalasit, A., Barone, S. and Petrucci, G. (1995) Automated photoelasticity in white light: influence of quarter wave plates. *J. Strain Anal.* **30**, 29–34.
12. Zandman, F., Redner, S. and Dally, J. W. (1977) *Photoelastic Coatings*. Society for Experimental Stress Analysis (SESA) monograph. SESA, Iowa.
13. Yoneyama, S., Shimizu, M., Gotoh, J. and Takashi, M. (1998) Photoelastic analysis with a single tricolor image. *Opt. Lasers Eng.* **29**, 423–435.
14. Ng, T. W., Quek, P. K. and Lim, K. H. (2003) Phase-shifting photoelasticity using a flatbed scanner. *Opt. Eng.* **42**, 2375–2379.
15. Hoy, D. E. P. (1998) A color scanner as a digital recording polariscope. *Exp. Tech.* **22**, 26–27.

